

Sol-Gel Preparation and Characterization of Nanocomposite Sr-Substituted $\text{La}_{1-x}\text{Sr}_x\text{CoO}_3$ Perovskite Type Materials

Anjali B. Bodade, Swati M. Ghodsal, Archana B. Bodade, Gajanan N. Chaudhari*

Nanotechnology Research Laboratory, Department of Chemistry, Shri. Shivaji Science College,
Amravati, M.S, India

ABSTRACT: Nanocomposites $\text{La}_{1-x}\text{Sr}_x\text{CoO}_3$ material was synthesized by sol gel technique and calcined with different temperatures. The structural characterizations of synthesized by X-ray diffraction, scanning electron microscopy, energy dispersive X-ray analysis and Fourier transform infrared spectra and electric properties were investigated by impedance spectroscopy. The diffraction patterns of X-ray diffraction characterization indicates that the average particle size of the nanocrystalline $\text{La}_{0.9}\text{Sr}_{0.1}\text{CoO}_3$ is in the range of 30-35 nm. The frequency dependent dielectric dispersion of nanocomposites Sr doped LaCoO_3 nanomaterials were investigated by impedance spectroscopy. The Impedance plots were used as tools to analyse the sample behaviour as a function of frequency, Cole–Cole plots and Nyquist Plot of $\text{La}_{1-x}\text{Sr}_x\text{CoO}_3$ were studied.

KEYWORDS: LaCoO_3 , Sol-gel method, Structural Characterization, dielectric properties.

I. INTRODUCTION

Perovskite-type metal oxides with general formula ABO_3 may potentially replace noble metal catalysts due to their high activity, thermal stability, and low costs [1]. The catalytic properties of ABO_3 basically depend on the nature of A and B ions. Therefore, the electronic properties and catalytic activity of the perovskite-type oxides can be modified by substitution of other heterovalent ions into the A or B sites [2]. Perovskite type metal oxides exhibit extremely high selectivity for oxygen due to the existence of oxygen vacancy. This is mainly because the A-site doping alkaline earth metal ions increase the concentration of oxygen vacancies, and the B-site doping transition metal ions produce mixed valence[3].

The perovskite-type oxides are non-toxic, easily handled and mild oxidizing catalysts. Despite of several advantages over traditional catalysts, they have been less explored in organic synthesis. In this study we report the effects on the structural and electrical phenomena caused by the doping of trivalent (Sr^{3+}) cations on LaCoO_3 synthesized by the sol-gel method. LaCoO_3 doped with various metal ions such as Li- and Sr[4], Mg, Ca- and Sr[5], Ca[6], Co [7], Sm^{3+} and Sr^{2+} [8], Cu-, Ni- and V [9], and Fe [10] were previously studied. The sol gel synthesized nanomaterials relies on the ability to obtain a homogeneous distribution of cations at the atomic scale and a uniform size in the nanometer range, with a simple technique that does not require high temperature and vacuum. The synthesized $\text{La}_{1-x}\text{Sr}_x\text{CoO}_3$ ($x=0, 0.1$) were studied using XRD, FTIR, SEM, EDAX, impedance spectroscopy in order to study the structural and electrical properties.

International Journal of Innovative Research in Science, Engineering and Technology

(A High Impact Factor, Monthly, Peer Reviewed Journal)

Visit: www.ijirset.com

Vol. 8, Issue 9, September 2019

II. EXPERIMENTAL

Nanocrystalline $\text{La}_{1-x}\text{Sr}_x\text{CoO}_3$ were prepared using sol-gel method[1]. High purity nitrates were used for the preparation. A stoichiometric mixture cerium nitrate and zirconium nitrate were used as raw materials. A stoichiometric mixture of nit rates was mixed with equal amount of citric acid and 30 ml ethanol and stirred magnetically on hot plate at 80°C for 3h to obtain a homogenous mixture; the solution was further heated in a pressure vessel at about 130°C for 12 hrs and subsequently kept at 350°C for 3 hrs in muffle furnace and then milled to a fine powder. The dried powder was then calcined in the range of 350°C to 750°C for 6 hrs in order to improve the crystallinity and surface morphology and porosity. The morphology and size of the resulting nanomaterial was examined using Scanning Electron Microscopy (SEM). The phase of the nanomaterial was identified by X-ray Diffraction (XRD). The impedance measurements were done on the pellets (the pellets of 13.2 mm diameter and 15.45 mm thickness were made by applying a pressure of 8 tons on the powered sample) by using an LCR meter. Impedance measurement were carried out in the frequency range 42 Hz-500 MHz and at temperature range 37 to 700°C [11]

III. RESULT AND DISCUSSION

3.1 X-ray diffraction study

The XRD patterns of the nanocomposites LaCoO_3 and $\text{La}_{1-x}\text{Sr}_x\text{CoO}_3$ ($x = 0, 0.1$) prepared by sol-gel method calcined at 650°C shown in Fig 1.. Fig. 1(A) shows XRD pattern of LaCoO_3 which is in good agreement with XRD results previously reported in the literature for LaCoO_3 [12]. All the diffraction peaks of the phases are indexed as perovskite-type with tetragonal structure. Fig. 1(B), shows the XRD pattern of $\text{La}_{1-x}\text{Sr}_x\text{CoO}_3$ ($x = 0.1$) nanomaterial. Extremely broad reflections are observed indicating nanosized particle nature of the material obtained. The mean crystallite sizes (D) of $\text{La}_{1-x}\text{Sr}_x\text{CoO}_3$ ($x = 0, 0.1$) powder was deduced from half height width of XRD peaks based on the Scherrer's equation, $D = 0.9\lambda/\beta\cos\theta$, where D is the average size of the particles, λ is wavelength of X-ray radiation, β the full width at half maximum of the diffracted peak and θ is the angle of diffraction[13]. The average particle size of the nanocrystalline $\text{La}_{1-x}\text{Sr}_x\text{CoO}_3$ ($x = 0, 0.1$) according to the Scherrer's formula was in the range of 30–35 nm.

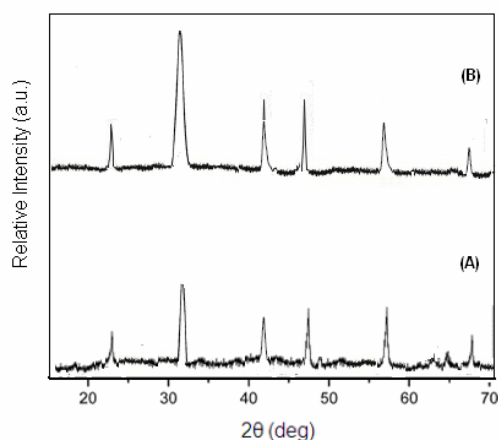


Fig1. X-ray diffraction pattern of the synthesized nanocomposite $\text{La}_{1-x}\text{Sr}_x\text{CoO}_3$

(A) $x = 0$ (B) $x = 0.1$) calcined at 650°C .

3.2 FTIR Analysis

Fig. 2 shows FTIR of sol-gel synthesized nanocomposites $\text{La}_{0.9}\text{Sr}_{0.1}\text{CoO}_3$. The FTIR spectrum of the LaCoO_3 powder has three characteristic bands at 412.78 cm^{-1} , 594.10 cm^{-1} and 659.68 cm^{-1} . The two strong absorption bands at about 594.10 cm^{-1} and 659.68 cm^{-1} are assigned to Co-O stretching vibration and O-Co-O deformation modes of LaCoO_3 , respectively [14-17]. La-O bond was assigned to the presence of the absorption band at around $415\text{--}423\text{ cm}^{-1}$ [18].

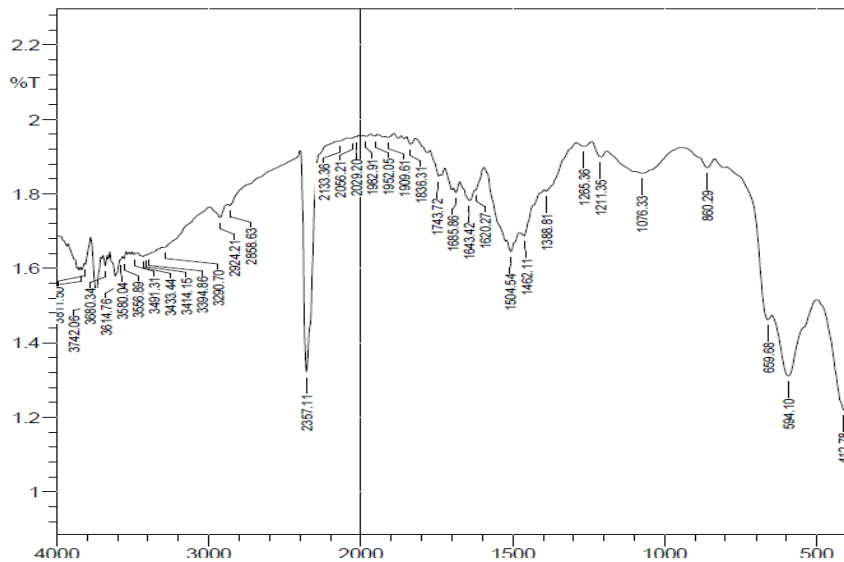


Fig. 2. FT-IR spectrum of nanocomposite $\text{La}_{0.9}\text{Sr}_{0.1}\text{CoO}_3$

3.3 SEM analysis

Fig.3 shows the microstructure of nanocomposites $\text{La}_{0.9}\text{Sr}_{0.1}\text{CoO}_3$ consisting of grains of Sr substituted LaCoO_3 . This shows more porosity, giving largest effective surface area. SEM of $\text{La}_{0.9}\text{Sr}_{0.1}\text{CoO}_3$ nanocomposites prepared by sol-gel method shows uniform with some agglomeration of the nanoparticles were observed. The sizes of the particles, determined from the SEM micrograph, is in the order of $30\text{--}35\text{ nm}$. These values of particle size are in good acceptance with the particle size calculated by Scherrer's formula.

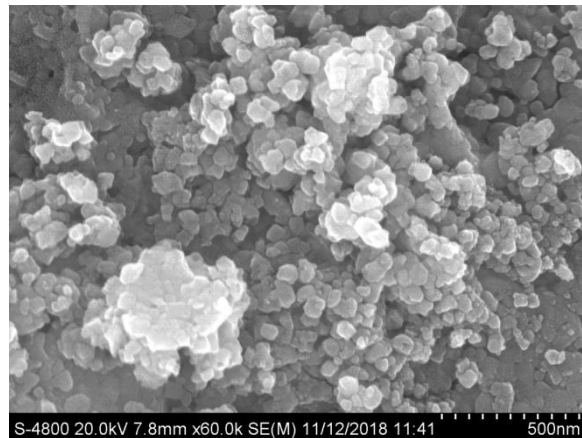


Fig.3 SEM micrograph of nanocomposites $\text{La}_{0.9}\text{Sr}_{0.1}\text{CoO}_3$

3.4 Energy Dispersive X-ray (EDAX) Spectroscopy Analysis

The chemical composition of compounds was confirmed from the EDAX spectrum. Fig. 4 shows that the atomic weight percentages of various cations in the as synthesized nanocomposites were found to be approximately correct which corresponds to a composition ratio and these ratios are expected.

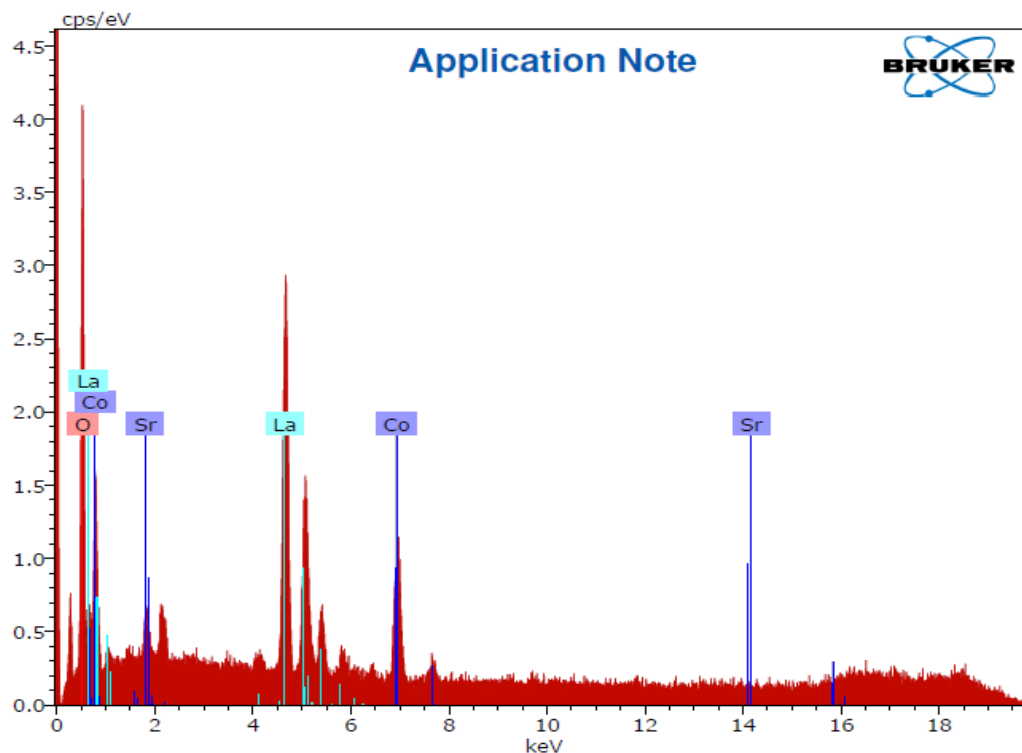


Fig. 4. EDAX pattern of $\text{La}_{0.9}\text{Sr}_{0.1}\text{CoO}_3$ nanocomposites

IV. ELECTRICAL PROPERTIES

Impedance spectral analysis

Electrical Impedance Spectroscopy (EIS) is a technique used in a wide range of applications. Electrical impedance or simply impedance, describes a measure of opposition to alternating current (a.c.). In this, AC impedance measurements are made over a wide range of frequencies and the different regions of the material are characterized according to their electrical relaxation times or time constants. Impedance spectroscopy is relatively easy to use and is applicable to a wide variety of materials and problems. A complex impedance spectrum of ceramic sample shows two distinct features intragrain (grain) and intergrain (grain boundary). Impedance data are presented in the form of Z'' (capacitive) and Z' (resistive).

Fig 5(b) shows the imaginary part of impedance (Z'') for $\text{La}_{0.9}\text{Sr}_{0.1}\text{CoO}_3$ nanocomposites. At low temperatures below 150°C , the value of Z'' is high at low frequency and decreases with the increase of frequency indicating that electric relaxations are absent.

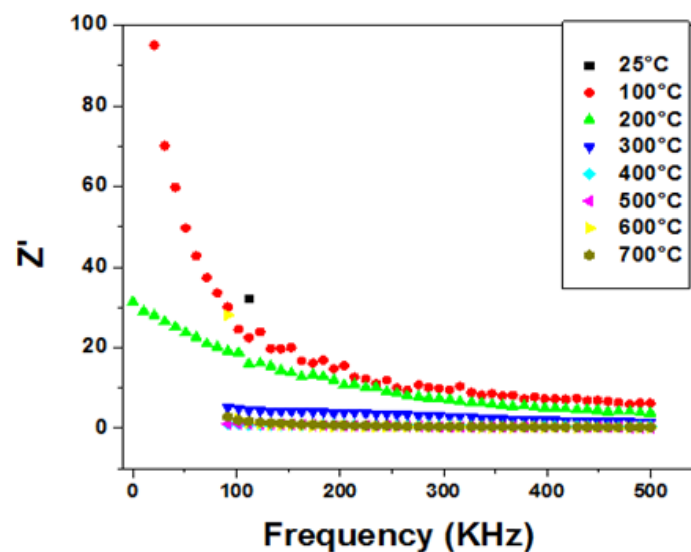


Fig 5 (a): Frequency dependence of real part of impedance (Z') for $\text{La}_{0.9}\text{Sr}_{0.1}\text{CoO}_3$ nanocomposites

Fig. 5 (a) shows the response of the real components of impedance (Z') with frequency for $\text{La}_{0.9}\text{Sr}_{0.1}\text{CoO}_3$ nanocomposites at different temperature. It is observed that at lower frequency range, the magnitude of Z' (grain resistance) decreases with rise in temperature and appears to merge in the high frequency region. This may be due to the release of space charge polarization with rise in temperature and frequency [19].

International Journal of Innovative Research in Science, Engineering and Technology

(A High Impact Factor, Monthly, Peer Reviewed Journal)

Visit: www.ijirset.com

Vol. 8, Issue 9, September 2019

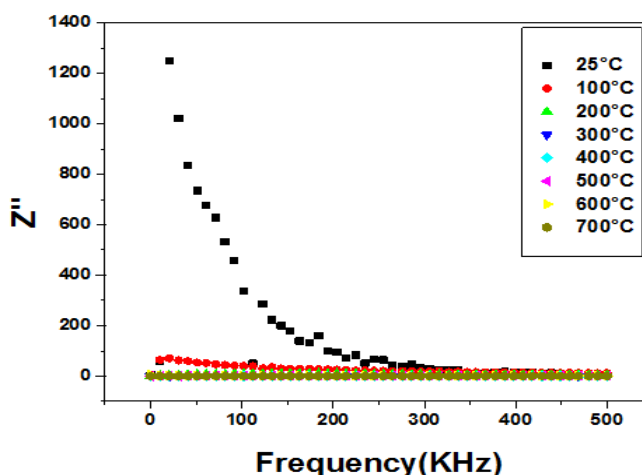


Fig 5 (b) : Frequencydependence of imaginary part of impedance (Z'') for $\text{La}_{0.9}\text{Sr}_{0.1}\text{CoO}_3$ nanocomposites

Fig 5(b) shows the imaginary part of impedance (Z'') for $\text{La}_{0.9}\text{Sr}_{0.1}\text{CoO}_3$ nanocomposites. At low temperatures below 150°C , the value of Z'' is high at low frequency and decreases with the increase of frequency indicating that electric relaxations are absent.

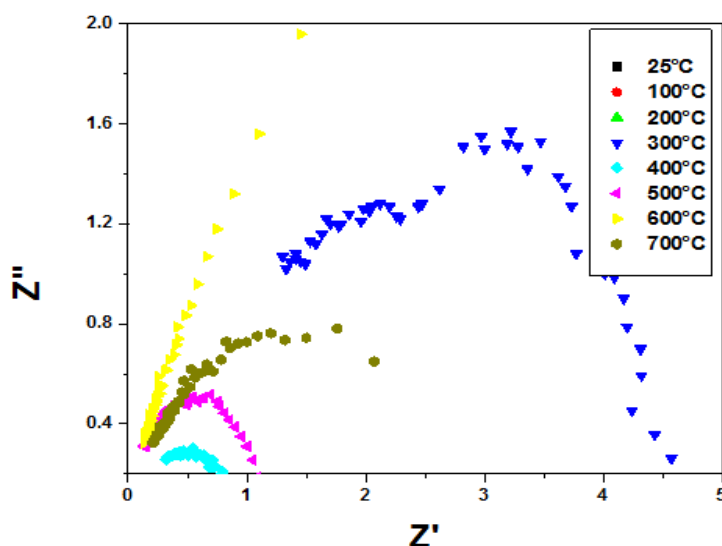


Fig.5(c).Nyquist Plot of $\text{La}_{0.9}\text{Sr}_{0.1}\text{CoO}_3$

Fig 5(c) shows Nyquist plot of $\text{La}_{0.9}\text{Sr}_{0.1}\text{CoO}_3$ at different temperatures. These plot allow resistances related to grain interiors (bulk), grain boundaries and sample/electrode interfaces to be separated because each of them has different relaxation times. The analysis of these semicircular arcs gives, from the high frequency side, the grain-bulk, the grain-

International Journal of Innovative Research in Science, Engineering and Technology

(A High Impact Factor, Monthly, Peer Reviewed Journal)

Visit: www.ijirset.com

Vol. 8, Issue 9, September 2019

boundary. All these semicircles are not perfect semicircles, but inclined with their centers below the Z' –Axis by an angle, which is different for each case.

V. CONCLUSION

Nanocrystalline $\text{La}_{1-x}\text{Sr}_x\text{CoO}_3$ ($x=0.0.1$) has been synthesized by a convenient sol–gel route. The XRD pattern of $\text{La}_{0.9}\text{Sr}_{0.1}\text{CoO}_3$ shows perovskite-type with tetragonal structure. The XRD results revealed that the particle size is in the range of 30–35 nm for $\text{La}_{0.9}\text{Sr}_{0.1}\text{CoO}_3$ with good crystallinity. FTIR shows two broad bands at 594.10 cm^{-1} and 659.68 cm^{-1} which indicate Co-O and O-Co-O stretching. The size of the particles, determined from the FE-SEM micrograph, is in the order of 30–35 nm. The chemical composition of compounds was confirmed from the EDAX spectrum. The value of Z' is higher at lower frequency region and as frequency increases the value of decreases. The value of Z'' is high at low frequency and decreases with the increase of frequency indicating that electric relaxations are absent. Impedance analysis indicated the presence of grain and grain boundary effect.

ACKNOWLEDGEMENT

The authors are thankful to Principal, Shri Shivaji Science College, Amravati (MS) for providing all research facilities during research work.

REFERENCES

- [1] Nyamdavaa Erdenee, Uyanga Enkhnanan, Sevjiduren Galsan, and Altantsog Pagvajav, "Lanthanum-Based Perovskite-Type Oxides $\text{La}_{1-x}\text{Ce}_x\text{BO}_3$ (B = Mn and Co) as Catalysts: Synthesis and Characterization" *Journal of Nanomaterials*, Vol 7, Issue 8, 2017
- [2] Mohammad G., Houshang A. H "Electrical and CO gas sensing properties of nanostructured $\text{La}_{1-x}\text{Ce}_x\text{CoO}_3$ perovskite prepared by activated reactive synthesis" *Sensors and Actuators*, Vol .156, pp. 147-155, 2011.
- [3] Tianyu Li, Rishvi S. Jayatilake, Daniel D. Taylor and Efrain E. Rodriguez, "Structural studies of perovskite $\text{La}_{1-x}\text{Sr}_x\text{CoO}_{3-\delta}$ during chemical looping with methane", *Chem. Commun.*, Vol 55, pp 4929-4932, 2019.
- [4] H.P.S. Correa, C.O. Paiva-Santos, L.F. Setz, L.G. Martinez, S.R.H. Mello-Castanho, M.T.D. Orlando, "Crystal structure refinement of Co-doped lanthanum chromites", *Powder Diffr. Suppl.*, Vol 23, S18, 2008.
- [5] S.M. El-Sheikh, M.M. Rashad, "Effect of Sm^{3+} and Sr^{2+} dopants on the FT-IR, "photoluminescence and surface texture of lanthanum chromite nanoparticles" *J. Alloys Compd*, Vol 496, pp723–73, 2010
- [6] G.-Y. Lee, R. H. Song, J.-H. Kim, D.-Y. Peck, T.-H. Lim, Y.-G. Shul, D.-R. Shin, "Properties of Cu, Ni, and V doped- LaCrO_3 interconnect materials prepared by Pechini, ultrasonic spray pyrolysis and glycine nitrate processes for SOFC", *J. Electroceram*, Vol 17, pp 723–727, 2006.
- [7] W. Hu, Y. Ch, R.J.H. Voorhoeve, *Advanced Materials in Catalysis*, Academic Press, New York, 1977
- [8] E. Suda, B. Pacaud, T. Seguelong, Y. Takeda, "Sintering characteristics and thermal expansion behavior of Li-doped lanthanum chromite perovskites depending upon preparation method and Sr doping", *Solid State Ionics*, Vol 151, pp 335–34, 2002.
- [9] M. Mori, T. Yamamoto, T. Ichikawa, Y. Takeda, "Dense sintered conditions and sintering mechanism for alkaline earth metal (Mg,Ca, and Sr) – doped LaCrO_3 perovskite under reducing atmosphere", *Solid State Ionics*, Vol 148, pp 93–101, 2002.
- [10] N. Sakai, T. Kawada, H. Yokokawa, M. Dokiya, T. Iwata, "Sinterability and electrical conductivity of calcium-doped lanthanum chromites", *J. Mater. Sci.*, Vol 25, 1990.
- [11] V.D. Nithya, R. Jacob Immanuel, S.T. Senthilkumar, C. Sanjeeviraja, I. Perelshtein, D. Zitoun, R. Kalai Selvan, "Studies on the structural, electrical and magnetic properties of LaCrO_3 , $\text{LaCr}_{0.5}\text{Cu}_{0.5}\text{O}_3$ and $\text{LaCr}_{0.5}\text{Fe}_{0.5}\text{O}_3$ by sol–gel method", *Materials Research Bulletin*, Vol 47, pp 1861–1868, 2012
- [12] M.M. Fukate, A.B. Bodade, G.N. Chaudahry, "Efficient Nanostructure Cathode Material for Low Temperature Solid Oxide Fuel Cells: $\text{LaSr}_{0.5}\text{Mn}_{0.5}\text{Co}_{2-x}\text{Fe}_x\text{O}_{5+\delta}$ ", *Nano Trends* Vol 19, Issue 3, pp 49-55, 2017
- [13] M. Mori, T. Yamamoto, T. Ichikawa, Y. Takeda, "Dense sintered conditions and sintering mechanism for alkaline earth metal (Mg,Ca, and Sr) – doped LaCrO_3 perovskite under reducing atmosphere", *Solid State Ionics*, Vol 148, pp 93–101, 2002.
- [14] N. Sakai, T. Kawada, H. Yokokawa, M. Dokiya, T. Iwata, "Sinterability and electrical conductivity of calcium-doped lanthanum chromites", *J. Mater. Sci.*, Vol 25, 1990.
- [15] X. Ding, Y. Liu, L. Gao and L. Guo, *J. Alloys Compd.*, 458, 346–350, 2008.
- [16] B. D. Cullity, *In Elements of X-ray Diffraction*, 2nd Edition, Addison Wesley, pp 155-165, 1978
- [17] A. Worayingyong, P. Kangvansura, S. Kityakarn, "Pure and Ca-doped LaCoO_3 Nanopowders: Sol-Gel Synthesis, Characterization and Magnetic synthesis", *Colloid Surface A: Physicochem.Eng. Aspects*, Vol 320, Issue 123, 2008.
- [18] E. Bontempi, L. Armelao, D. Barreca, L. Bertolo, G. Bottaro, E. Pierangelo, L.E. Depero, "Structural characterization of sol –gel lanthanum cobaltite thin film", *Crystal Eng.*, Vol 5, Issue 291, 2002.
- [19] C. Matei, D. Berger, P. Marote, S. Stoleriu, J. Deloume, "Lanthanum based perovskite obtained in molten nitrates or nitrites", *Prog. Solid State Chem.*, Vol 35, Issue 203, 2007.